Published in final edited form as:
Diabetes. 2017 March 31; 66(4): 897–907. doi:10.2337/db16-0336.

Loss of $\alpha_2\delta$-1 Calcium Channel Subunit Function Increases the Susceptibility for Diabetes

Vincenzo Mastrolia[1,2], **Sylvia M. Flucher**[1], **Gerald J. Obermair**[1], **Mathias Drach**[3], **Helene Hofer**[1], **Erik Renström**[4], **Arnold Schwartz**[5], **Jörg Striessnig**[2], **Bernhard E. Flucher**[1], **Petronel Tuluc**[1,2]

[1]Department of Physiology and Medical Physics, Medical University Innsbruck, Innsbruck, Austria

[2]Department of Pharmacology and Toxicology, Institute of Pharmacy, University of Innsbruck, Innsbruck, Austria

[3]Department of General Pathology, Medical University Innsbruck, Innsbruck, Austria

[4]Department of Clinical Sciences Malmö, Lund University, Lund, Sweden

[5]College of Medicine, University of Cincinnati, Cincinnati, OH

Abstract

Reduced pancreatic β-cell function or mass is the critical problem in developing diabetes. Insulin release from β-cells depends on Ca^{2+} influx through high voltage– gated Ca^{2+} channels (HVCCs). Ca^{2+} influx also regulates insulin synthesis and insulin granule priming and contributes to β-cell electrical activity. The HVCCs are multisubunit protein complexes composed of a pore-forming $\alpha 1$ and auxiliary β and $\alpha_2\delta$ subunits. $\alpha_2\delta$ is a key regulator of membrane incorporation and function of HVCCs. Here we show that genetic deletion of $\alpha_2\delta$-1, the dominant $\alpha_2\delta$ subunit in pancreatic islets, results in glucose intolerance and diabetes without affecting insulin sensitivity. Lack of the $\alpha_2\delta$-1 subunit reduces the Ca^{2+} currents through all HVCC isoforms expressed in β-cells equally in male and female mice. The reduced Ca^{2+} influx alters the kinetics and amplitude of the global Ca^{2+} response to glucose in pancreatic islets and significantly reduces insulin release in both sexes. The progression of diabetes in males is aggravated by a selective loss of β-cell mass, while a stronger basal insulin release alleviates the diabetes symptoms in most $\alpha_2\delta\text{-}1^{-/-}$ female mice. Together, these findings demonstrate that the loss of the Ca^{2+} channel $\alpha_2\delta$-1 subunit function increases the susceptibility for developing diabetes in a sex-dependent manner.

In response to elevated blood glucose levels, pancreatic β-cells release insulin by a Ca^{2+} channel–dependent process, with a rapidly rising transient first phase followed by a

Corresponding authors: Petronel Tuluc, petronel.tuluc@uibk.ac.at, and Bernhard E. Flucher, bernhard.e.flucher@i-med.ac.at.

Duality of Interest. No potential conflicts of interest relevant to this article were reported.

Author Contributions. V.M. performed experiments, designed research, and wrote the manuscript. S.M.F., M.D., and H.H. performed experiments. G.J.O., E.R., and J.S. provided expertise and feedback. A.S. provided the KO mouse model. B.E.F. and P.T. performed experiments, designed research, wrote the manuscript, and acquired funding. P.T. is the guarantor of this work and, as such, had full access to all the data in the study and takes responsibility for the integrity of the data and the accuracy of the data analysis.

Europe PMC Funders Author Manuscripts

sustained second release phase (1). Pharmacological block or genetic deletion demonstrated that $Ca_V1.2$ channels are responsible for insulin release in the first and second phase (2–4). $Ca_V1.2$ Ca^{2+} currents are also critical for shaping the electrical activity of pancreatic β-cells, and in the absence of $Ca_V1.2$ channels, the fast phase of insulin release is strongly delayed (2,5). Conversely, gain-of-function mutations in $Ca_V1.2$ channels lead to hypoglycemia and death (6). Genetic ablation of $Ca_V1.3$ channels has been shown to reduce the postnatal generation and survival of mouse β-cells (7), and human genetic polymorphisms reducing $Ca_V1.3$ expression increase the susceptibility for type 2 diabetes (8). R-type Ca^{2+} currents through $Ca_V2.3$ channels have been proposed to be necessary for the priming of insulin granules at the plasma membrane and thus for sustaining the tonic second-phase insulin release (9,10). Therefore, the tight control of Ca^{2+} entry through multiple high voltage–gated Ca^{2+} channels (HVCCs) is of critical importance for normal β-cell function and for the maintenance of β-cell mass in pancreatic islets. Any alteration in the composition and function of HVCCs is expected to lead to β-cell dysfunction and diabetes (11,12).

HVCCs are heteromeric membrane proteins composed of a pore-forming α_1-subunit, an intracellular β-subunit, and an extracellular $\alpha_2\delta$-subunit (13,14). The role of $\alpha_2\delta$-1 in the channel complex can vary, depending on the tissue in which it is expressed and on the specific α_1-isoform with which it associates. In neurons, the primary role of $\alpha_2\delta$-1 is to promote the plasma membrane incorporation of Ca_V1 and Ca_V2 channels (15–18), whereas in muscle cells, the $\alpha_2\delta$-1 subunit determines the characteristic current kinetics of $Ca_V1.1$ and $Ca_V1.2$ channels (19–21). Recent transcriptome analysis indicated that $\alpha_2\delta$-1 is the main $\alpha_2\delta$-isoform expressed in both human and mouse pancreatic islets (22). Several loss-of-function mutations in the CACNA2D1 gene have been identified that associate with epilepsy and intellectual disability (23), short QT syndromes (24,25), and cardiac arrhythmias (26). However, the physiological role of $\alpha_2\delta$-1 in endocrine cells is unknown and its importance for HVCC channel function in β-cells, on dynamic insulin release and glucose tolerance, has not been analyzed.

Here, we show that the constitutive knockout (KO) of the $\alpha_2\delta$-1 Ca^{2+} channel subunit (27) results in reduced first- and second-phase insulin release, in both male and female mice, without affecting the insulin sensitivity. A stronger basal insulin release partially alleviates the diabetes symptoms in most $\alpha_2\delta$-$1^{-/-}$ females. However in $\alpha_2\delta$-$1^{-/-}$ males and to a much lower extent in $\alpha_2\delta$-$1^{-/-}$ females, a selective and progressive loss in β-cell mass, secondary to diabetes, amplifies the symptoms. Collectively, our data show that impaired $\alpha_2\delta$-1 function leads to diabetes in males and increases diabetes susceptibility in females. This critical role of the Ca^{2+} channel $\alpha_2\delta$-1 subunit in normal blood sugar regulation should prompt clinical studies investigating glucose tolerance in patients carrying CACNA2D1 loss-of-function mutations (23–26).

Research Design and Methods

$\alpha_2\delta$-$1^{-/-}$ Mice

$\alpha_2\delta$-$1^{-/-}$ mouse strain was previously generated and characterized (27,28). In the previous reports, the $\alpha_2\delta$-$1^{-/-}$ mice were bred in a C57BL/6 genetic background, whereas our colony has a mixed C57BL/6 × 129J background. $\alpha_2\delta$-$1^{+/+}$ and $\alpha_2\delta$-$1^{-/-}$ littermates were bred from

heterozygous mice. All experiments were performed on 4- to 5-week-old animals unless stated otherwise. All animal experiments were performed in conformity with international laws and were approved by the Austrian Ministry of Science (BMWFW-66.008/0015-WF/V/3b/2014).

Immunohistochemistry

Males—After dissection, the pancreas was fixed overnight in buffered 4% paraformaldehyde and subsequently embedded in paraffin. Serial 4-μm-thick sections were stained with hematoxylin and eosin, for insulin (A0564, dilution 1:100; DAKO) and for glucagon (PA5-32424, dilution 1:50; Thermo Fisher Scientific). Islet numbers were determined by counting all islets in every sixth section of the whole pancreas. The islet size was calculated by integrating the area of at least 20 islets per mouse.

Females—Pancreas was perfused with 4% paraformaldehyde, stored overnight in 4% paraformaldehyde at 4°C, and subsequently prepared for cryopreservation: 30% sucrose in PBS (overnight, 4°C), 30% OCT (2 h, 4°C, Tissue-Tek; Sakura Finetek Europe B.V.), 100% OCT (1 h, 4°C), −20°C in the cryostat. Sections were cut 20 μm thick and stained for insulin (A0564 1/1,000 + Alexa568 [DAKO] and Ab175714, 1/4,000 [Abcam]) and glucagon (G2654, 1/200 + Alexa488 [Sigma-Aldrich] and A11029, 1/2,000 [Thermo Fisher Scientific]). Islet and cells numbers were counted in every section.

Isolation of Pancreatic Islets and β-Cells

Pancreatic islets were enzymatically isolated as previously reported (9). For Ca^{2+} fluorometry and insulin release, islets were cultured at 37°C for 2 h in RPMI1640 medium supplemented with 10% FCS, 2 mmol/L L-glutamine, 5 mmol/L glucose, 100 μg/mL streptomycin, and 100 IU/mL penicillin. To disperse the pancreatic cells, the islets were incubated in solution containing (mmol/L) 138 NaCl, 6 KCl, 3 $MgCl_2$, 5 HEPES, 3 glucose, 1 EGTA, and 1 mg/mL BSA for 10 min at 37°C and then mechanically dissociated. Single cells were cultured for at least 3 h in RPMI1640 medium before the start of the experiment.

Electrophysiology

Ionic currents were recorded from dispersed pancreatic islet cells using perforated-patch technique at room temperature using the Axopatch 200B amplifier. To record Ca^{2+} currents, the pipette solution contained (mmol/L) 76 $CsSO_4$, 10 CsCl, 10 KCl, 1 $MgCl_2$, and 5 HEPES with 120 μg/mL amphotericin B (Sigma-Aldrich), and the extracellular solution contained (mmol/L) 140 TEA-Cl, 5.6 KCl, 1.2 $MgCl_2$, 5 HEPES, 2.6 $CaCl_2$, and 5 glucose. To pharmacologically dissect the contribution of different HVCC isoforms to total β-cell Ca^{2+} currents, we used isradipine (2 μmol/L), a $Ca_V1.2$ and $Ca_V1.3$ L-type Ca^{2+} channel blocker, and SNX-482 (100 nmol/L), a $Ca_V2.3$ R-type channel blocker. For recording sodium currents and capacitance increase, the extracellular solution contained also (mmol/L) 138 NaCl and 20 TEA-Cl. The voltage dependence of the sodium current inactivation was used to identify β-cells (29). The increase in cell capacitance after step depolarizations was recorded at 32°C using the lock-in sine+DC mode of HEKA amplifier controlled by the PULSE software.

Ca^{2+} Fluorometry

Isolated pancreatic islets were loaded with Indo-1 Ca^{2+} indicator (6 μmol/L; Invitrogen) for 1 h at room temperature, followed by 30 min at 37°C. Single islets were perfused with 37°C solution ([mmol/L] 140 NaCl, 0.5 NaH_2PO_4, 0.5 $MgSO_4$-$7H_2O$, 2.5 $CaCl_2$, 2 $NaHCO_3$, 5 HEPES, 3.6 KCl) with a perfusion rate of 2 mL/min. Fluorescent signals (400 and 480 nm) were recorded using two photomultipliers (PTI, South Brunswick, NJ).

Dynamic Insulin Release and Insulin Content

For each animal, a group of 20 islets of similar size were perfused with the same solution as for Ca^{2+} imaging at 250 μL/min flow rate, and the insulin concentration of the 2-min fractions was measured with either a normal sensitive ($\alpha_2\delta$-$1^{+/+}$ mice) or an ultrasensitive ($\alpha_2\delta$-$1^{-/-}$ mice) ELISA kit (Mercodia). The insulin content was extracted from groups of 10 islets using the acid-ethanol method (2,9).

Quantitative TaqMan PCR

Total RNA was extracted from isolated islets using the RNeasy Mini kit (Qiagen) and reverse transcribed (SuperScriptII; Invitrogen). The relative abundance of $\alpha_2\delta$ isoforms was assessed by TaqMan quantitative PCR (50 cycles) using a standard curve based on PCR products of known concentrations and normalization to endogenous controls (30,31). TaqMan gene expression assays were purchased from Applied Biosystems (31).

Statistical Analysis

Data analysis was performed using Clampfit 10.2 (Axon Instruments), Sigma Plot 11 (Systat Software, Inc.), Excel 11 (Microsoft), or GraphPad Prism 7. All values are presented as mean ± SE for the indicated number of experiments (*n*), except if stated otherwise. Statistical significance was calculated using unpaired Student *t* test (Welch test for differing variances) or one-way ANOVA followed by Bonferroni post hoc test as indicated.

Results

All $\alpha_2\delta$-$1^{-/-}$ Males and Some $\alpha_2\delta$-$1^{-/-}$ Female Mice Have Altered Metabolic Parameters and Shorter Life Span

The original characterization of the $\alpha_2\delta$-$1^{-/-}$ mouse reported decreased basal myocardial contractility and relaxation due to altered $Ca_V1.2$ Ca^{2+} influx. Otherwise, $\alpha_2\delta$-$1^{-/-}$ mice appeared normal, except that KO males displayed a tendency for bladder dilatation (27) (A. Schwartz, personal communication). Indeed, anatomical reexamination showed severely enlarged bladders and kidneys, especially in KO males >2 months of age (Fig. 1A). These symptoms were accompanied by a dramatic increase in water consumption and urine excretion (Fig. 1B and C, solid lines). In contrast, most KO females showed no signs of bladder extension, increased water consumption, or urine excretion. However, when affected (one out of five females examined in metabolic cages), the severity of the symptoms in KO females was comparable to that of the males (Fig. 1B, red dotted line).

Deletion of $\alpha_2\delta$-1 did not affect the survival rate in utero, as the genotype of newborn mice of heterozygous parents followed a Mendelian ratio (Fig. 1D). However, postnatal survival

of KO males declined rapidly (Fig. 1E), with <50% of mice surviving at 5 months of age (16 out of 41, survival rate 39%). In contrast, the survival rate of the KO females (93%) was hardly affected, as out of 41 females, only 3 were symptomatic and died within 1 year. Together these symptoms strongly indicated that a progressive diabetic phenotype reduced survival rate, especially in males.

$\alpha_2\delta$-1$^{-/-}$ Mice Are Glucose Intolerant But Insulin Sensitive

Indeed, KO males on average had approximately threefold higher basal blood glucose levels at 1 month, increasing to approximately ninefold at 5 months of age (Fig. 2A). Young KO females (1 month of age) had modestly elevated basal blood glucose levels compared with their wild-type (WT) littermates, but glucose levels normalized as the mice matured (Fig. 2A). Intraperitoneal glucose tolerance test (IPGTT) in 6 h–fasted mice clearly demonstrated abnormal glucose tolerance for both KO males and females, although to a different extent. In WT males, blood glucose levels increased by approximately twofold 15 min after glucose injection (1g/kg, i.p.) and then returned to fasting levels within 1 h. In KO males, the same dose of glucose raised blood glucose levels to values approximately three times higher than in WT mice and their blood glucose levels did not normalize even after 2 h. $\alpha_2\delta$-1 deletion also strongly reduced glucose tolerance in females. However, both WT and KO females cleared glucose significantly faster than the corresponding males (Fig. 2B).

Because skeletal muscle, the primary tissue regarding glucose utilization, expresses high levels of $\alpha_2\delta$-1, we next examined insulin sensitivity in WT and KO mice after 6 h fasting. Within 30 min after injection of insulin (0.75 units/kg, i.p.), plasma glucose levels were lowered to the same concentration in KO and WT mice (Fig. 2C). This indicated that general KO of $\alpha_2\delta$-1 did not result in reduced insulin sensitivity, pointing to pancreatic islet dysfunction as a cause for the glucose intolerance in $\alpha_2\delta$-1$^{-/-}$ mice. This possibility was substantiated by our quantitative qRT-PCR data, which show that $\alpha_2\delta$-1 is by far the dominant $\alpha_2\delta$ isoform in pancreatic islets and that genetic ablation of $\alpha_2\delta$-1 is not compensated by a comparable upregulation of $\alpha_2\delta$-2 or -3 transcripts (Fig. 2D).

$\alpha_2\delta$-1$^{-/-}$ Males Show a Progressive Reduction in β-Cell Mass

To quantify possible effects of $\alpha_2\delta$-1 KO on the number, size, and composition of pancreatic islets, we immunolabeled pancreas sections from 6- and 14-week-old males and 15–18-week-old females with antibodies against insulin and glucagon. In 6-week-old WT and KO males, the insulin-positive β-cells occupied the core of the pancreatic islet whereas glucagon-positive a-cells surrounded them in the periphery (Fig. 3A). At 14 weeks of age, the $\alpha_2\delta$-1$^{-/-}$ male islets had fewer insulin-positive β-cells (Fig. 3B). Quantification of the islet density revealed a small nonsignificant reduction at 6 weeks (Fig. 3C), and their average size was normal (Fig. 3D). However, in 14-week-old KO mice, the islet density was significantly reduced by 66% (Fig. 3C), and this was accompanied by a 46% reduction in islet size and almost complete loss of larger islet profiles (Fig. 3D).

To examine whether the reduction in the islet size is caused by specific loss of β-cells, we quantified the density of α- and β-cells (Fig. 3E and F). Whereas the β-cell density was significantly decreased in KO compared with WT islets at 6 and 14 weeks of age, the α-cell

density did not decline. Thus, whereas severe hyperglycemia was observed in 4-week-old $\alpha_2\delta$-$1^{-/-}$ males (compared with Fig. 2), pancreatic islets initially developed normally. To examine whether deletion of $\alpha_2\delta$-1 alters the β-cell mass in the absence of severe diabetes symptoms, we performed a similar analysis in nonsymptomatic 15–18-week-old females. In $\alpha_2\delta$-$1^{-/-}$ females, the structure of the islet was intact (Fig. 3G), whereas the surface area of the islet was rather increased by 24% (Fig. 3H). The β-cell density was decreased by 9.7% (Fig. 3I), but the α-cell numbers increased by 42% in $\alpha_2\delta$-$1^{-/-}$ islets compared to WT (Fig. 3J).

Knockout of $\alpha_2\delta$-1 Reduces Ca^{2+} Influx in Pancreatic β-Cells Equally in Females and Males

To identify the molecular mechanism responsible for hyperglycemia, we first analyzed the properties of the HVCC Ca^{2+} currents in dissociated pancreatic β-cells (9). Whole-cell patch-clamp recordings revealed greatly diminished Ca^{2+} currents in male and female $\alpha_2\delta$-$1^{-/-}$ mice (Fig. 4A and G). The I/V curves (current-voltage relationship) showed an ~70% reduced mean maximal current density in both KO males and females (Fig. 4B and H), whereas the voltage dependence of activation was not significantly changed (Fig. 4C and I). Furthermore, the Ca^{2+} currents recorded from $\alpha_2\delta$-$1^{-/-}$ β-cells displayed altered kinetic properties (Fig. 4A and G) with a significantly slowed activation time course (time to peak) in males (from 5.2 ± 0.2 to 8.4 ± 1.0 ms) and females (5.9 ± 0.3 to 8.8 ± 1.1 ms) (Fig. 4D and J). The fractional inactivation after 200 ms was also significantly reduced in both males (from 63.1 ± 2.3% to 45 ± 5.1%) (Fig. 4F) and females (from 63.2 ± 2.7% to 46.3 ± 4.2%) (Fig. 4L), but not after 50 ms (Fig. 4E and K). Therefore, the lack of $\alpha_2\delta$-1 equally affects Ca^{2+} influx in β-cells of male and female KO mice.

All HVCC Types Are Equally Reduced in $\alpha_2\delta$-$1^{-/-}$ β-Cells

Several different HVCC isoforms contribute to β-cell function (11,32). Application of the L-type Ca^{2+} channel blocker isradipine (2 μmol/L) reduced the β-cell current density by ~70% (Fig. 5A–C). Additional application of the $Ca_V2.3$ channel blocker SNX-482 (100 nmol/L) further reduced the current density by 15% of total. The remaining ~15% current corresponds to P/Q- and N-type (Ca_V2) channels (2). The smaller Ca^{2+} currents in $\alpha_2\delta$-$1^{-/-}$ β-cells were blocked by isradipine (~70%) and SNX-482 (~15%) to similar extents (Fig. 5D–F). This shows that the genetic deletion of $\alpha_2\delta$-1 does not alter the fractional contribution of L- and R-type currents in β-cells.

Knockout of $\alpha_2\delta$-1 Differentially Alters the Ca^{2+} Dynamics in Pancreatic Islets of Male and Female Mice

How do reduced current density and slowed inactivation of Ca^{2+} currents alter glucose-induced Ca^{2+} signals in the $\alpha_2\delta$-$1^{-/-}$ pancreatic islets? To answer this question, we loaded isolated pancreatic islets with the ratiometric Ca^{2+} indicator Indo-1 (6 μmol/L) and recorded the fluorescent signal from whole islets (9). In 5 mmol/L extracellular glucose, the pancreatic islets showed stable resting fluorescence levels. One minute after increasing glucose to 15 mmol/L, a strong rise in cytoplasmic free Ca^{2+} concentration ($[Ca^{2+}]i$) was recorded in all islets (Fig. 6A and E). However, the time to peak of the first-phase Ca^{2+} response was more than doubled in $\alpha_2\delta$-$1^{-/-}$ islets of both sexes compared with controls

(Fig. 6B and F). Moreover, in male $\alpha_2\delta$-$1^{-/-}$ islets, the magnitude of the glucose-induced Ca^{2+} transient was significantly smaller compared with the WT islets (Fig. 6C and D).

To bypass possible alterations in glucose metabolism or excitability of $\alpha_2\delta$-$1^{-/-}$ β-cells, we applied the K_{ATP} channel blocker tolbutamide (100 μmol/L) (33,34). The $[Ca^{2+}]$i transient in response to tolbutamide was also substantially decreased in male $\alpha_2\delta$-$1^{-/-}$ islets compared with WT controls. Whereas the female $\alpha_2\delta$-$1^{-/-}$ islets displayed significantly slowed activation of the first-phase glucose response, the amplitude of the glucose- or tolbutamide-induced $[Ca^{2+}]$i transient increase was not reduced (Fig. 6G and H). Passive depolarization with 50 mmol/L KCl induced a significantly lower $[Ca^{2+}]$i peak in $\alpha_2\delta$-$1^{-/-}$ islets of both sexes compared with WT controls. To investigate whether altered intracellular Ca^{2+} store load contributes to reduced islet $[Ca^{2+}]$i peak in male islets, we stimulated the Ca^{2+} release via InsP3R (inositol triphosphate receptor) with 1 μmmol/L carbachol (Fig. 6I and J). Whereas the amplitude of the KCl step was significantly reduced in $\alpha_2\delta$-$1^{-/-}$ islets (WT 0.76 6 0.03, KO 0.37 6 0.01), the amplitude of the carbachol-induced $[Ca^{2+}]$i transient was similar for both WT (0.37 6 0.02, $n = 20$) and $\alpha_2\delta$-$1^{-/-}$ islets (0.38 6 0.02, $n = 26$). Taken together, the $[Ca^{2+}]$i recordings in isolated islets demonstrate that the loss of $\alpha_2\delta$-1 function results in a severely delayed $[Ca^{2+}]$i response and also in males a smaller amplitude and total integrated $[Ca^{2+}]$i responses. The reduced $[Ca^{2+}]$i transient is caused by reduced Ca^{2+} influx and not by altered intracellular store release.

$\alpha_2\delta$-1 Deletion Drastically Reduces Insulin Release but Not Insulin Content of Pancreatic Islets

Because in $\alpha_2\delta$-$1^{-/-}$ mice the Ca^{2+} influx through L-type and R-type HVCCs is dramatically reduced (Figs. 4 and 5) and the first-phase islet $[Ca^{2+}]$i transient is substantially delayed (Fig. 6), we expected a change in the dynamics of insulin release. To measure this, we perfused 20 isolated islets and collected fractions every 2 min for analysis of insulin concentration. As expected, after increasing from 5 to 15 mmol/L glucose, WT islets responded with a fast peak of insulin release followed by a smaller sustained release phase. At the end of the experiment, massive insulin release was induced by passively depolarizing the islets with KCl (50 mmol/L). In WT females, but not in males, the second-phase insulin release steadily increased to levels above the initial peak (Fig. 6A and E). The distinct phases of insulin release were observed in both WT and $\alpha_2\delta$-$1^{-/-}$ islets. However, $\alpha_2\delta$-1 deletion substantially reduced all phases of insulin release in islets of both sexes. In $\alpha_2\delta$-$1^{-/-}$ male islets, the maximal amplitude of the first phase was reduced by 78% (Fig. 6B) and the integral of the second phase by 77% (Fig. 6C). Peak KCl-induced release was reduced by 51%. In female islets, the amplitude of the first phase was reduced by 60%, integrated insulin secreted during the slow phase by 77%, and the peak of KCl-induced insulin release by 61% (Fig. 6F and G). Notably, these differences were not due to different insulin content in islets from WT and KO mice (Fig. 7D and H). To probe whether the reduced islet insulin release is caused by impaired β-cell secretory function, we quantified the increase in membrane capacitance after 10 consecutive 500-ms depolarization steps in male β-cells (Fig. 7I). In $\alpha_2\delta$-$1^{-/-}$ β-cells, the average capacitance at the end of the stimulus train was 179.9 ± 17.9 fF ($n = 24$) and in WT cells 519.5 ± 52.3 fF ($n = 25$) (Fig. 7J). The increase in membrane capacitance after the first depolarization step, reflecting the ready releasable pool

of insulin vesicles, was significantly smaller in $\alpha_2\delta$-$1^{-/-}$ β-cells (17.6 ± 6.6 fF) compared with WT β-cells (64.9 ± 17.9 fF) (Fig. 7K). The average increase in membrane capacitance induced by each subsequent depolarization step was also significantly reduced as the $\alpha_2\delta$-$1^{-/-}$ β-cell capacitance increased by only 22.6 ± 1.9 fF and that of WT β-cells by 51.1 ± 4.9 fF (Fig. 7L).

Surprisingly, both the fast and slow phases of insulin release from female (WT or $\alpha_2\delta$-$1^{-/-}$) islets were significantly higher than insulin release from male islets of the same genotype. As a consequence, $\alpha_2\delta$-$1^{-/-}$ female islets (Fig. 7E–G, red) secrete more than twice as much insulin as $\alpha_2\delta$-$1^{-/-}$ male islets in response to glucose (integral of insulin release: WT females 135.8 ± 20.2, males 60.1 ± 10.2, $P = 0.007$; $\alpha_2\delta$-$1^{-/-}$ females 34.25 ± 7.3, males 14.5 ± 2.7, $P = 0.04$).

Discussion

A broad spectrum of symptoms and tested parameters demonstrate that loss of $\alpha_2\delta$-1 Ca^{2+} channel subunit increases the susceptibility to diabetes in mice. Consistent with the role of $\alpha_2\delta$-1 in functional membrane expression of Ca^{2+} channel shown in other cell types (35–37), our data show that Ca^{2+} influx is equally reduced in β-cells of both sexes. In KO males, this results in reduced insulin release and in an escalation of diabetes with severe β-cell loss. Whereas a more robust insulin release in female mice enables most KO females to cope with the reduced Ca^{2+} signal, and to sufficiently regulate blood glucose levels and maintain β-cell mass. The finding that an indiscriminate reduction of Ca^{2+} currents of all HVCC isoforms of β-cells leads to a complex sex-specific diabetes phenotype is novel. Similar to the situation in human diabetes, genetic variations affecting the basal efficiency of insulin release (38) contributes to the manifestation of diabetes in the $\alpha_2\delta$-$1^{-/-}$ mice. This could also explain why an overt diabetic phenotype has not been noted up to 12 weeks of age, in an $\alpha_2\delta$-$1^{-/-}$ mouse colony on a C57BL/6J genetic background (28) (A.C. Dolphin, personal communication).

As demonstrated here for mice, also in human pancreatic islets, $\alpha_2\delta$-1 is the dominant $\alpha_2\delta$ subunit isoform (22,39,40). Although several genomic aberrations of the CACNA2D1 gene have been associated with epilepsy and intellectual disability (23), short QT syndromes (24), and cardiac arrhythmias (26), the role of $\alpha_2\delta$ subunits in diabetes has hitherto not been analyzed in these patients. Our current findings suggest that patients carrying CACNA2D1 loss-of-function mutations, in particular males, should be closely monitored for impaired glucose tolerance.

Primary Cause of Diabetes in $\alpha_2\delta$-$1^{-/-}$ Mice Is β-Cell Dysfunction

Several lines of evidence indicate that the primary cause of diabetes in $\alpha_2\delta$-$1^{-/-}$ mice is reduced insulin secretion. Ca^{2+} currents in $\alpha_2\delta$-$1^{-/-}$ β-cells and Ca^{2+} influx–induced exocytosis are reduced. The first phase of the glucose-induced $[Ca^{2+}]i$ signal in $\alpha_2\delta$-$1^{-/-}$ islets is delayed and the glucose-induced insulin release is reduced not only in affected $\alpha_2\delta$-$1^{-/-}$ males but also in unaffected females and in young mice prior to the development of severe clinical signs. In theory, the general KO of the $\alpha_2\delta$-1 subunit could also affect glucose regulation by islet-independent mechanisms. In particular, in skeletal muscle, where

Europe PMC Funders Author Manuscripts

$\alpha_2\delta$-1 is the exclusive $\alpha_2\delta$-1 isoform, its KO might impair the regulation of glucose uptake. However, in $\alpha_2\delta$-$1^{-/-}$ mice, insulin sensitivity was not different from normal controls.

Another cause for diabetes in $\alpha_2\delta$-$1^{-/-}$ mice could be reduced β-cell mass due to impaired β-cell neogenesis or survival. However, our data show that in young males and older asymptomatic females, the number of pancreatic islets is not affected (Fig. 3A–D), indicating that impaired generation or postnatal survival of β-cells cannot be the primary cause of the reduced insulin release. The dramatic loss of β-cells in older males is most probably secondary to impaired insulin release and blood glucose regulation (41). Furthermore, if the $\alpha_2\delta$-1 subunit is required for pancreatic endocrine cell survival, then an equal reduction of a-cells would be expected in $\alpha_2\delta$-$1^{-/-}$ males, which was not observed.

$\alpha_2\delta$-1 Knockout Causes Reduced Ca^{2+} Currents Through All HVCC Isoforms

Our observation that a substantial reduction of Ca^{2+} currents occurred in β-cells of young $\alpha_2\delta$-$1^{-/-}$ mice and that a similar current reduction was seen in asymptomatic females excludes the possibility that this effect on the Ca^{2+} currents was the result, rather than the cause, of diabetes (42). In pancreatic islets of the $\alpha_2\delta$-$1^{-/-}$ mice, the upregulation of $\alpha_2\delta$-2 and -3 transcripts is way too small to quantitatively compensate for the loss of $\alpha_2\delta$-1. Our data also suggest that in normal β-cells, all HVCC types associate with the $\alpha_2\delta$-1 isoform since the $\alpha_2\delta$-1 KO equally reduces Ca^{2+} currents carried by all examined HVCC types. Moreover, the requirement of $\alpha_2\delta$-1 for the membrane expression of multiple HVCCs also explains the complex effects of $\alpha_2\delta$-1 KO on the different phases of Ca^{2+} dynamics and insulin secretion.

$\alpha_2\delta$-1 Deletion Alters Ca^{2+} Dynamics and Reduces First- and Second-Phase Insulin Secretion

$Ca_V1.2$ channel activation is required for insulin vesicle fusion (3) and critically contributes to the initiation of electrical activity in β-cells (2), whereas the activation of $Ca_V2.3$ channels plays a role in maintaining the Ca^{2+} signaling and insulin release in the slow-sustained second phase (9,10). Consistent with the importance of $\alpha_2\delta$-1 for the function of both of these HVCCs, the Ca^{2+} dynamics of the first phase was significantly retarded and both phases of insulin release were strongly reduced in islets of KO males and females. Strikingly, in male $\alpha_2\delta$-$1^{-/-}$ islets, the reduction of Ca^{2+} dynamics and insulin release was greater in magnitude compared with what has earlier been demonstrated for male $Ca_V1.2^{-/-}$ or $Ca_V2.3^{-/-}$ mouse models alone (2,9). As $\alpha_2\delta$-1 appears to be the common constituent of multiple HVCCs in β-cells, its loss has more severe consequences than that of an individual HVCC α_1-subunit, and consequently genetic defects of $\alpha_2\delta$-1 in patients may have more detrimental effects on blood glucose regulation than the loss of function of a single pore-forming HVCC subunit.

Although both phases of insulin release and the first-phase Ca^{2+} signal were equally affected in KO males and females in response to a glucose challenge, the strong sex difference in the Ca^{2+} dynamics and insulin release in the WT animals explains the lower incidence of diabetes in KO females. First, the second-phase Ca^{2+} signal was not different in $\alpha_2\delta$-$1^{-/-}$ and WT females. Notably, this type of measurement does not reflect Ca^{2+} dynamics of

single β-cells but the complex spatio-temporal spread of the Ca^{2+} signal through the entire islet (43,44). Second, female islets secrete more insulin than male islets, and even though the $\alpha_2\delta$-1 deletion strongly reduced insulin release in both sexes, the remaining release in female KO is similar to that in WT males and appears to be sufficient to regulate blood glucose levels and prevent β-cell loss and the escalation of the diabetic phenotype. This interpretation is consistent with the higher efficiency of glucose utilization in the IPGTT test in KO females compared with KO males. Our data also support the notion that the observed sex difference in the incidence of diabetes is caused by differences in β-cell function and is not a sex-specific metabolic phenomenon independent of the islet β-cell. The insulin sensitivity was not sex specific, and the differences in insulin release were observed in isolated islets therefore in the absence of any acute sex hormone regulation.

Conclusion

The current study demonstrates a key role of the $\alpha_2\delta$-1 HVCC subunit in insulin metabolism–secretion coupling. The $\alpha_2\delta$-1 subunit is required for proper β-cell Ca^{2+} influx through multiple HVCC isoforms, and its absence results in reduced insulin secretion and impaired glucose tolerance. Our findings highlight that the control of HVCC currents by $\alpha_2\delta$-1 influences the in vivo insulin secretion and may have direct clinical relevance for patients carrying loss-of-function mutations in the CACNA2D1 gene (23,24,26).

Acknowledgments

The authors thank Gospava Stojanovic (Department of Pharmacology and Toxicology, University of Innsbruck) for excellent technical support.

Funding

This study was funded by grants from the Austrian Science Fund (P23479 and F4406 to B.E.F. and F4415 to G.J.O.) and the University of Innsbruck (P7400-027-011 and P7400-027-012 to P.T.).

References

1. Rorsman P, Eliasson L, Renström E, Gromada J, Barg S, Göpel S. The cell physiology of biphasic insulin secretion. News Physiol Sci. 2000; 15:72–77. [PubMed: 11390882]
2. Schulla V, Renström E, Feil R, et al. Impaired insulin secretion and glucose tolerance in beta cell-selective Ca(v)1.2 Ca2+ channel null mice. EMBO J. 2003; 22:3844–3854. [PubMed: 12881419]
3. Barg S, Ma X, Eliasson L, et al. Fast exocytosis with few Ca(2+) channels in insulin-secreting mouse pancreatic B cells. Biophys J. 2001; 81:3308–3323. [PubMed: 11720994]
4. Barg S, Eliasson L, Renström E, Rorsman P. A subset of 50 secretory granules in close contact with L-type Ca2+ channels accounts for first-phase insulin secretion in mouse beta-cells. Diabetes. 2002; 51(Suppl. 1):S74–S82. [PubMed: 11815462]
5. Sinnegger-Brauns MJ, Hetzenauer A, Huber IG, et al. Isoform-specific regulation of mood behavior and pancreatic beta cell and cardiovascular function by L-type Ca 2+ channels. J Clin Invest. 2004; 113:1430–1439. [PubMed: 15146240]
6. Splawski I, Timothy KW, Sharpe LM, et al. Ca(V)1.2 calcium channel dysfunction causes a multisystem disorder including arrhythmia and autism. Cell. 2004; 119:19–31. [PubMed: 15454078]
7. Namkung Y, Skrypnyk N, Jeong MJ, et al. Requirement for the L-type Ca(2+) channel alpha(1D) subunit in postnatal pancreatic beta cell generation. J Clin Invest. 2001; 108:1015–1022. [PubMed: 11581302]

8. Reinbothe TM, Alkayyali S, Ahlqvist E, et al. The human L-type calcium channel CaV1.3 regulates insulin release and polymorphisms in CACNA1D associate with type 2 diabetes. Diabetologia. 2013; 56:340–349. [PubMed: 23229155]
9. Jing X, Li DQ, Olofsson CS, et al. CaV2.3 calcium channels control second-phase insulin release. J Clin Invest. 2005; 115:146–154. [PubMed: 15630454]
10. Yang SN, Berggren PO. CaV2.3 channel and PKClambda: new players in insulin secretion. J Clin Invest. 2005; 115:16–20. [PubMed: 15630435]
11. Rorsman P, Braun M, Zhang Q. Regulation of calcium in pancreatic alpha- and beta-cells in health and disease. Cell Calcium. 2012; 51:300–308. [PubMed: 22177710]
12. Yang SN, Berggren PO. The role of voltage-gated calcium channels in pancreatic beta-cell physiology and pathophysiology. Endocr Rev. 2006; 27:621–676. [PubMed: 16868246]
13. Catterall WA. Structure and regulation of voltage-gated Ca2+ channels. Annu Rev Cell Dev Biol. 2000; 16:521–555. [PubMed: 11031246]
14. Zamponi GW, Striessnig J, Koschak A, Dolphin AC. The physiology, pathology, and pharmacology of voltage-gated calcium channels and their future therapeutic potential. Pharmacol Rev. 2015; 67:821–870. [PubMed: 26362469]
15. Bauer CS, Nieto-Rostro M, Rahman W, et al. The increased trafficking of the calcium channel subunit alpha2delta-1 to presynaptic terminals in neuropathic pain is inhibited by the alpha2delta ligand pregabalin. J Neurosci. 2009; 29:4076–4088. [PubMed: 19339603]
16. Dolphin AC. Calcium channel auxiliary α2δ and β subunits: trafficking and one step beyond. Nat Rev Neurosci. 2012; 13:542–555. [PubMed: 22805911]
17. Geisler S, Schöpf CL, Obermair GJ. Emerging evidence for specific neuronal functions of auxiliary calcium channel $\alpha_2\delta$ subunits. Gen Physiol Biophys. 2015; 34:105–118. [PubMed: 25504062]
18. Luo ZD, Calcutt NA, Higuera ES, et al. Injury type-specific calcium channel alpha 2 delta-1 subunit up-regulation in rat neuropathic pain models correlates with antiallodynic effects of gabapentin. J Pharmacol Exp Ther. 2002; 303:1199–1205. [PubMed: 12438544]
19. Obermair GJ, Kugler G, Baumgartner S, Tuluc P, Grabner M, Flucher BE. The Ca2+ channel alpha2delta-1 subunit determines Ca2+ current kinetics in skeletal muscle but not targeting of alpha1S or excitation-contraction coupling. J Biol Chem. 2005; 280:2229–2237. [PubMed: 15536090]
20. Tuluc P, Kern G, Obermair GJ, Flucher BE. Computer modeling of siRNA knockdown effects indicates an essential role of the Ca2+ channel alpha2delta-1 subunit in cardiac excitation-contraction coupling. Proc Natl Acad Sci USA. 2007; 104:11091–11096. [PubMed: 17563358]
21. Obermair GJ, Tuluc P, Flucher BE. Auxiliary Ca(2+) channel subunits: lessons learned from muscle. Curr Opin Pharmacol. 2008; 8:311–318. [PubMed: 18329337]
22. Benner C, van der Meulen T, Cacéres E, Tigyi K, Donaldson CJ, Huising MO. The transcriptional landscape of mouse beta cells compared to human beta cells reveals notable species differences in long non-coding RNA and protein-coding gene expression. BMC Genomics. 2014; 15:620. [PubMed: 25051960]
23. Vergult S, Dheedene A, Meurs A, et al. Genomic aberrations of the CACNA2D1 gene in three patients with epilepsy and intellectual disability. Eur J Hum Genet. 2015; 23:628–632. [PubMed: 25074461]
24. Templin C, Ghadri JR, Rougier JS, et al. Identification of a novel loss-of-function calcium channel gene mutation in short QT syndrome (SQTS6). Eur Heart J. 2011; 32:1077–1088. [PubMed: 21383000]
25. Burashnikov E, Pfeiffer R, Barajas-Martinez H, et al. Mutations in the cardiac L-type calcium channel associated with inherited J-wave syndromes and sudden cardiac death. Heart Rhythm. 2010; 7:1872–1882. [PubMed: 20817017]
26. Bourdin B, Shakeri B, Tetreault M, Sauve R, Lesage S, Parent L. Functional characterization of CaV alpha2delta mutations associated with sudden cardiac death. J Biol Chem. 2015; 290:2854–2869. [PubMed: 25527503]
27. Fuller-Bicer GA, Varadi G, Koch SE, et al. Targeted disruption of the voltage-dependent calcium channel alpha2/delta-1-subunit. Am J Physiol Heart Circ Physiol. 2009; 297:H117–H124. [PubMed: 19429829]

28. Patel R, Bauer CS, Nieto-Rostro M, et al. α2δ-1 gene deletion affects somatosensory neuron function and delays mechanical hypersensitivity in response to peripheral nerve damage. J Neurosci. 2013; 33:16412–16426. [PubMed: 24133248]
29. Göpel S, Kanno T, Barg S, Galvanovskis J, Rorsman P. Voltage-gated and resting membrane currents recorded from B-cells in intact mouse pancreatic islets. J Physiol. 1999; 521:717–728. [PubMed: 10601501]
30. Vandesompele J, De Preter K, Pattyn F, Poppe B, Van Roy N, De Paepe A, Speleman F. Accurate normalization of real-time quantitative RT-PCR data by geometric averaging of multiple internal control genes. Genome Biol. 2002; 3
31. Schlick B, Flucher BE, Obermair GJ. Voltage-activated calcium channel expression profiles in mouse brain and cultured hippocampal neurons. Neuroscience. 2010; 167:786–798. [PubMed: 20188150]
32. Braun M, Ramracheya R, Bengtsson M, et al. Voltage-gated ion channels in human pancreatic beta-cells: electrophysiological characterization and role in insulin secretion. Diabetes. 2008; 57:1618–1628. [PubMed: 18390794]
33. Trube G, Rorsman P, Ohno-Shosaku T. Opposite effects of tolbutamide and diazoxide on the ATP-dependent K+ channel in mouse pancreatic beta-cells. Pflugers Arch. 1986; 407:493–499. [PubMed: 2431383]
34. Arkhammar P, Nilsson T, Rorsman P, Berggren PO. Inhibition of ATP-regulated K+ channels precedes depolarization-induced increase in cytoplasmic free Ca2+ concentration in pancreatic beta-cells. J Biol Chem. 1987; 262:5448–5454. [PubMed: 2437108]
35. Davies A, Hendrich J, Van Minh AT, Wratten J, Douglas L, Dolphin AC. Functional biology of the alpha(2)delta subunits of voltage-gated calcium channels. Trends Pharmacol Sci. 2007; 28:220–228. [PubMed: 17403543]
36. Dolphin AC. The alpha(2)delta subunits of voltage-gated calcium channels. Biochim Biophys Acta. 2013; 1828:1541–1549. [PubMed: 23196350]
37. Hendrich J, Van Minh AT, Heblich F, et al. Pharmacological disruption of calcium channel trafficking by the {alpha}2{delta} ligand gabapentin. Proc Natl Acad Sci U S A. 2008; 105:3628–3633. [PubMed: 18299583]
38. Ashcroft FM, Rorsman P. Diabetes mellitus and the β cell: the last ten years. Cell. 2012; 148:1160–1171. [PubMed: 22424227]
39. Dorrell C, Schug J, Lin CF, et al. Transcriptomes of the major human pancreatic cell types. Diabetologia. 2011; 54:2832–2844. [PubMed: 21882062]
40. Fadista J, Vikman P, Laakso EO, et al. Global genomic and transcriptomic analysis of human pancreatic islets reveals novel genes influencing glucose metabolism. Proc Natl Acad Sci USA. 2014; 111:13924–13929. [PubMed: 25201977]
41. Poitout V, Robertson RP. Glucolipotoxicity: fuel excess and beta-cell dysfunction. Endocr Rev. 2008; 29:351–366. [PubMed: 18048763]
42. Roe MW, Philipson LH, Frangakis CJ, et al. Defective glucose-dependent endoplasmic reticulum Ca2+ sequestration in diabetic mouse islets of Langerhans. J Biol Chem. 1994; 269:18279–18282. [PubMed: 8034570]
43. Benninger RK, Zhang M, Head WS, Satin LS, Piston DW. Gap junction coupling and calcium waves in the pancreatic islet. Biophys J. 2008; 95:5048–5061. [PubMed: 18805925]
44. Stožer A, Gosak M, Dolenšek J, et al. Functional connectivity in islets of Langerhans from mouse pancreas tissue slices. PLOS Comput Biol. 2013; 9:e1002923. [PubMed: 23468610]

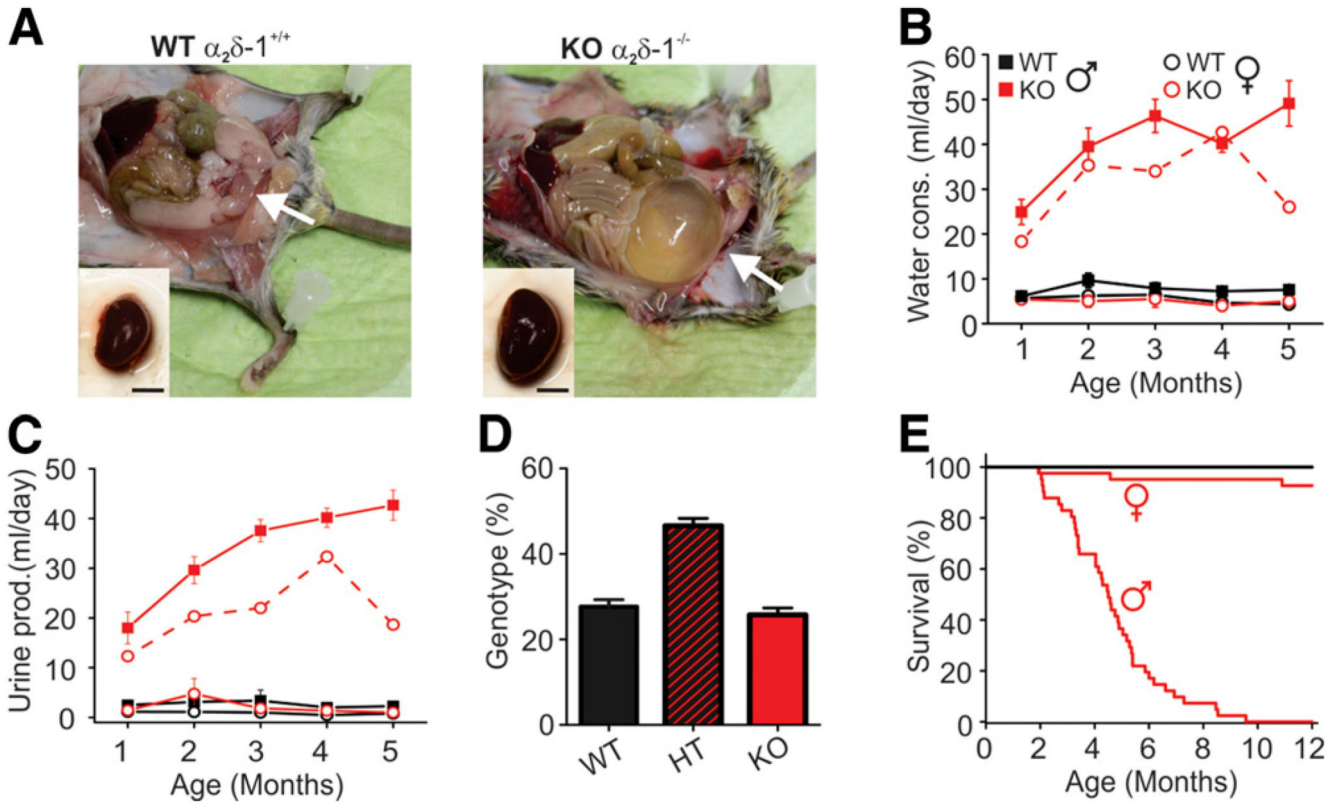

Figure 1.

Phenotypic characterization of $\alpha_2\delta$-1$^{-/-}$ mice. *A*: Adult $\alpha_2\delta$-1$^{-/-}$ males are lean and have enlarged bladder (arrows) and kidneys compared with their WT littermates (scale bar, 5 mm). Water consumption (*B*) and urine production (*C*) measured using metabolic cage (Tecniplast, Milan, Italy) ($n = 5$ of each sex and genotype). The dashed red line represents an example of a symptomatic female. *D*: Genotype of the newborn mice of heterozygous (HT) parents ($n > 450$). E: Postnatal survival rate of WT and $\alpha_2\delta$-1$^{-/-}$ mice ($n > 40$ of each sex and genotype).

Europe PMC Funders Author Manuscripts

Europe PMC Funders Author Manuscripts

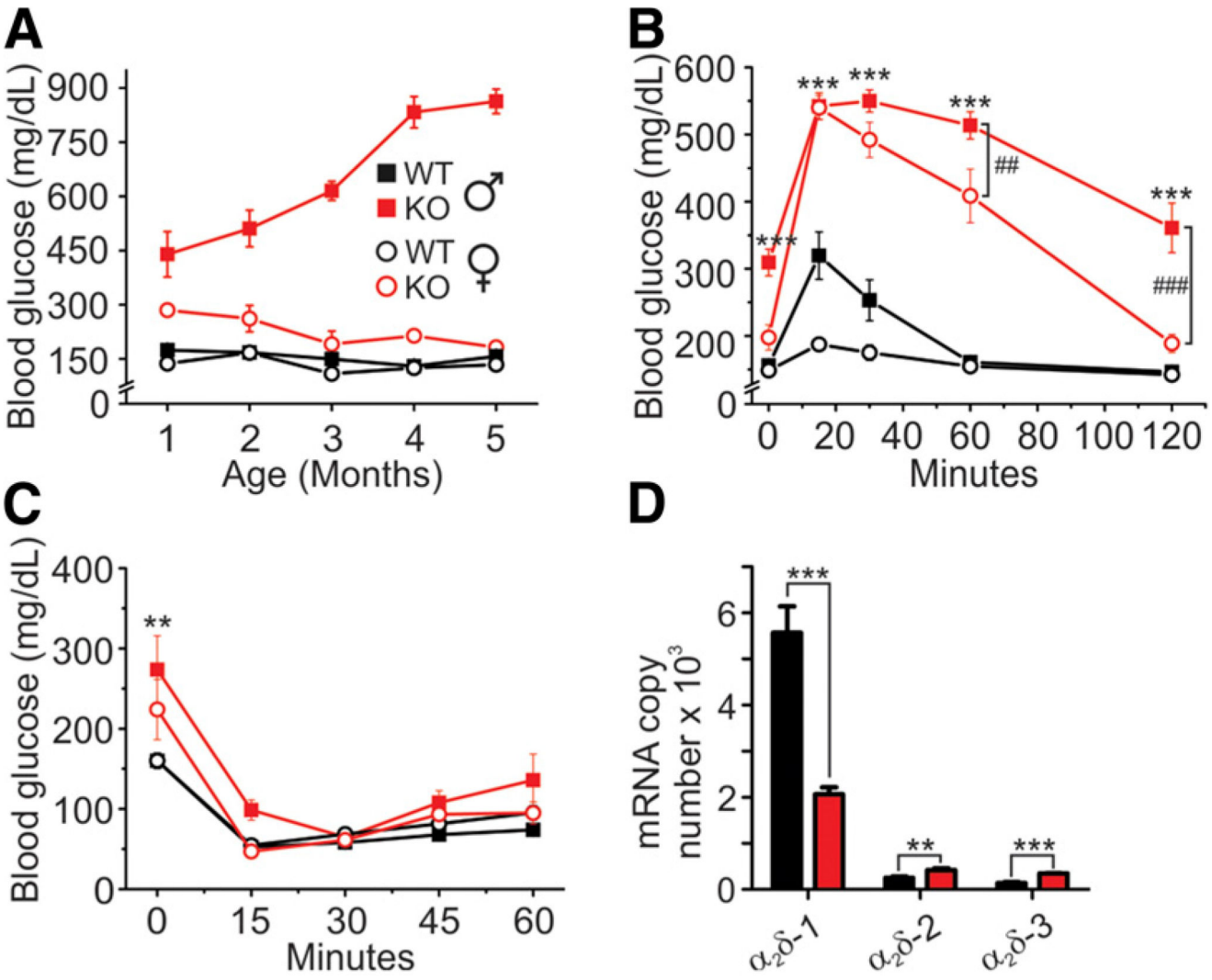

Figure 2.

$\alpha_2\delta$-1$^{-/-}$ mice are glucose intolerant but insulin sensitive. *A*: Nonfasting blood glucose levels in WT and $\alpha_2\delta$-1$^{-/-}$ mice ($n = 5$ of each sex and genotype). *B*: IPGTT using 1 mg/g body weight glucose (males WT $n = 6$, $\alpha_2\delta$-1$^{-/-}$ $n = 8$, females both genotypes $n = 7$). *C*: Intraperitoneal insulin sensitivity test after bovine insulin injection (0.75 units/kg body weight) (WT male $n = 4$, $\alpha_2\delta$-1$^{-/-}$ male $n = 9$, WT female $n = 10$, $\alpha_2\delta$-1$^{-/-}$ female $n = 7$). *D*: Quantitative real-time PCR analysis of $\alpha_2\delta$-1, -2, and -3 mRNA expression in isolated islets (WT $n = 3$, $\alpha_2\delta$-1$^{-/-}$ $n = 2$). All values are means ± SEM. Statistics with two-way ANOVA. $^{**}P < 0.01$, $^{***}P < 0.001$, comparison between WT and KO mice of the same sex; $^{\#\#}P < 0.01$, $^{\#\#\#}P < 0.001$, comparison between male and female KO mice.

Europe PMC Funders Author Manuscripts

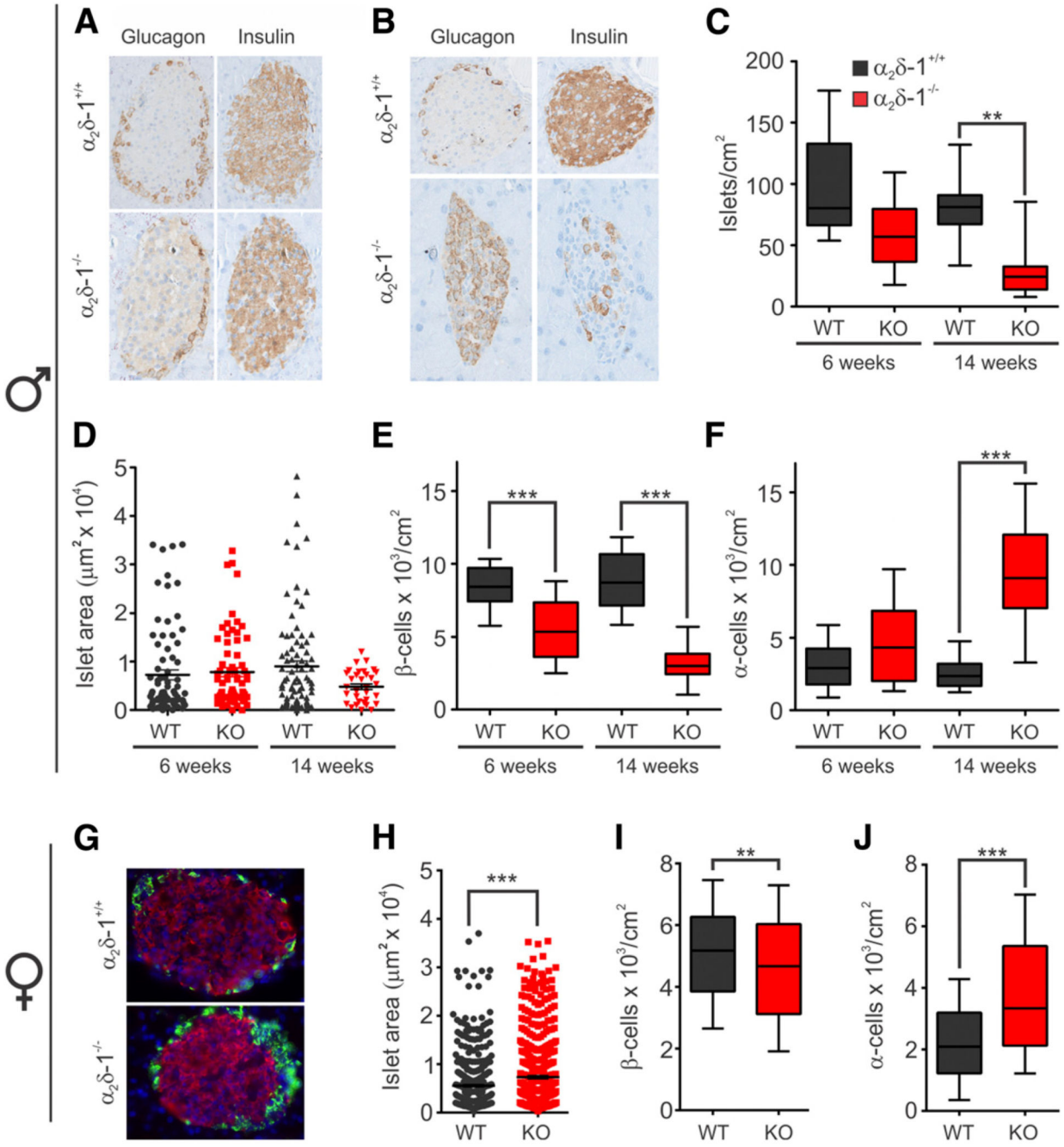

Figure 3.

$\alpha_2\delta$-$1^{-/-}$ deletion induces a progressive and selective loss of β-cells in males. *A*: Insulin and glucagon staining in fixed pancreatic sections from 6-week-old males ($n = 3$ both genotypes). *B*: Same as in A but at 14 weeks of age (WT $n = 5$; $\alpha_2\delta$-$1^{-/-}$ $n = 3$). *C*: Box plot analysis of the islet density in pancreatic sections from 6- and 14-week-old males. *D*: Dot plot indicating the islet size in the same pancreatic sections. Box plot depicting the β-cell density (*E*) and α-cell density (*F*) in islets of 6- and 14-week-old males. *G*: Insulin and glucagon staining in fixed pancreatic sections from 15- to 18-week-old females (WT $n = 2$,

$\alpha_2\delta$-$1^{-/-}$ $n = 3$). *H*: Dot plot indicating the islet size in the pancreatic sections from females. Box plot depicting the β-cell density (*I*) and α-cell density (*J*) in female islets. All values are means ± SEM. Statistics with Mann-Whitney nonparametric test: $^{**}P < 0.01$; $^{***}P < 0.001$.

Europe PMC Funders Author Manuscripts

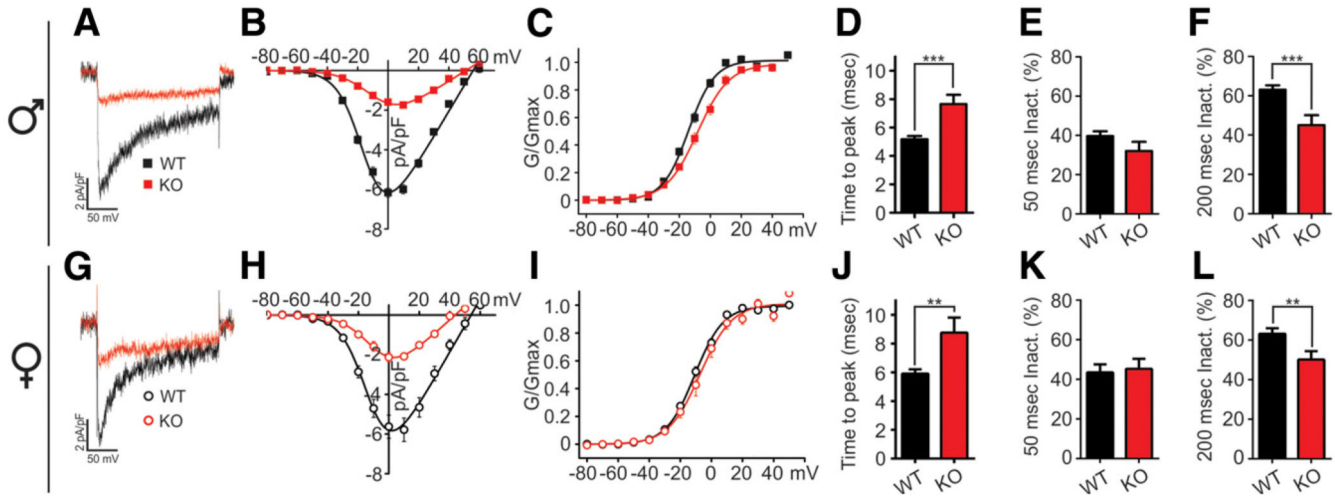

Figure 4.

β-Cell Ca^{2+} current density and kinetics are equally affected by $\alpha_2\delta$-1 deletion in both male and female mice. Representative Ca^{2+} current traces (*A* and *G*) and corresponding I/V curves (*B* and *H*) recorded in isolated β-cells of male (top) and female mice (bottom) ($\alpha_2\delta$-$1^{-/-}$ male and females $n = 13$, WT male $n = 22$, WT female $n = 16$). *C* and *I*: Voltage dependence of Ca^{2+} conductance. *D* and *J*: Activation kinetics (time to peak) of Ca^{2+} current. Fractional current inactivation after 50-ms (*E* and *K*) and 200-ms (*F* and *L*) depolarization. Ca^{2+} currents were elicited using 200-ms depolarization steps from −80 to +60 mV in 10-mV increments and analyzed as previously described (20). All values are means ± SEM. Statistics with Student *t* test: $^{**}P < 0.01$; $^{***}P < 0.001$.

Europe PMC Funders Author Manuscripts

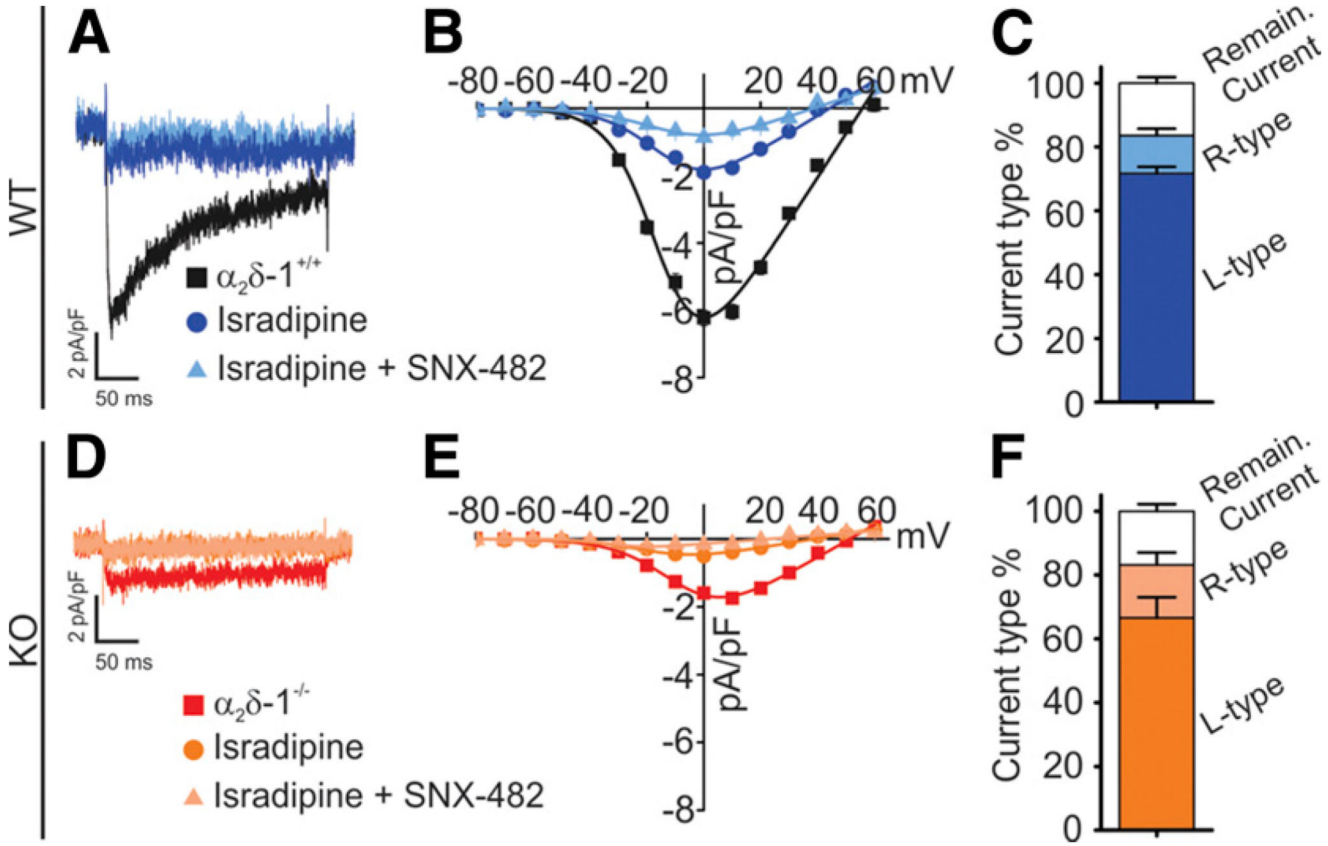

Figure 5.

Deletion of $\alpha_2\delta$-1 equally affects all β-cell HVCC isoforms. Sample recording of Ca^{2+} currents in WT male (*A*) and $\alpha_2\delta$-$1^{-/-}$ male (*D*) β-cells without drug application and after perfusion with 2 μmol/L isradipine or 2 μmol/L isradipine + 100 nmol/L SNX-482. I/V curve (*B* and *E*) and stack column (*C* and *F*) representation of the current density in the presence or absence of specific Ca^{2+} channel blockers. Ca^{2+} currents were elicited using 200-ms depolarization steps from −80 to +60 mV in 10-mV increments and analyzed as previously described (20). All values are means ± SEM. Statistics with Student *t* test.

Europe PMC Funders Author Manuscripts

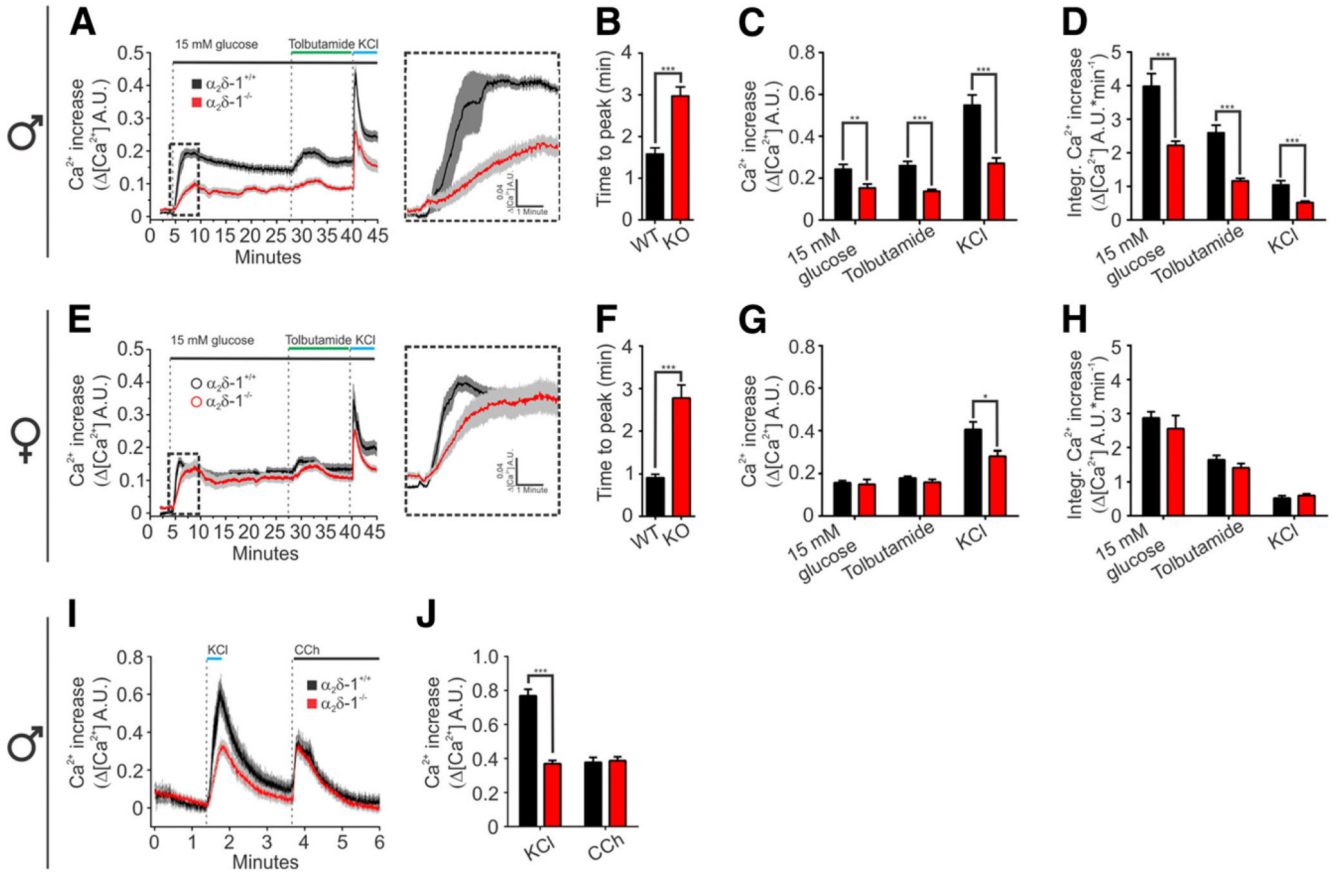

Figure 6.

Ca^{2+} transients are slower and have smaller amplitude in $\alpha_2\delta\text{-}1^{-/-}$ islets. Average Ca^{2+} transients in single islets isolated from male (*A*) and female (*E*) mice (male WT $n = 16$, $\alpha_2\delta\text{-}1^{-/-}$ $n = 15$, female WT $n = 14$, $\alpha_2\delta\text{-}1^{-/-}$ $n = 10$). The time to peak of the first phase in male islets (*B*) and female islets (*F*). The peak amplitudes (*C*) and integrals (*D*) of the glucose-dependent and glucose-independent Ca^{2+} transients in male islets. Amplitudes (*G*) and integrals (*H*) of the glucose-dependent and glucose-independent transients in female islets. *I*: Average $[Ca^{2+}]$i transients in single isolated male islets from WT ($n = 20$, four mice) and $\alpha_2\delta\text{-}1^{-/-}$ ($n = 26$, three mice) stimulated with 50 mmol/L KCl or 1 μmol/L carbachol (CCh). *J*: The average peak amplitude of the KCl and carbachol-induced $[Ca^{2+}]$i transients. All values are means ± SEM. Statistics with Student *t* test: *P < 0.05; **P < 0.01; ***P < 0.001. A.U., arbitrary units.

Europe PMC Funders Author Manuscripts

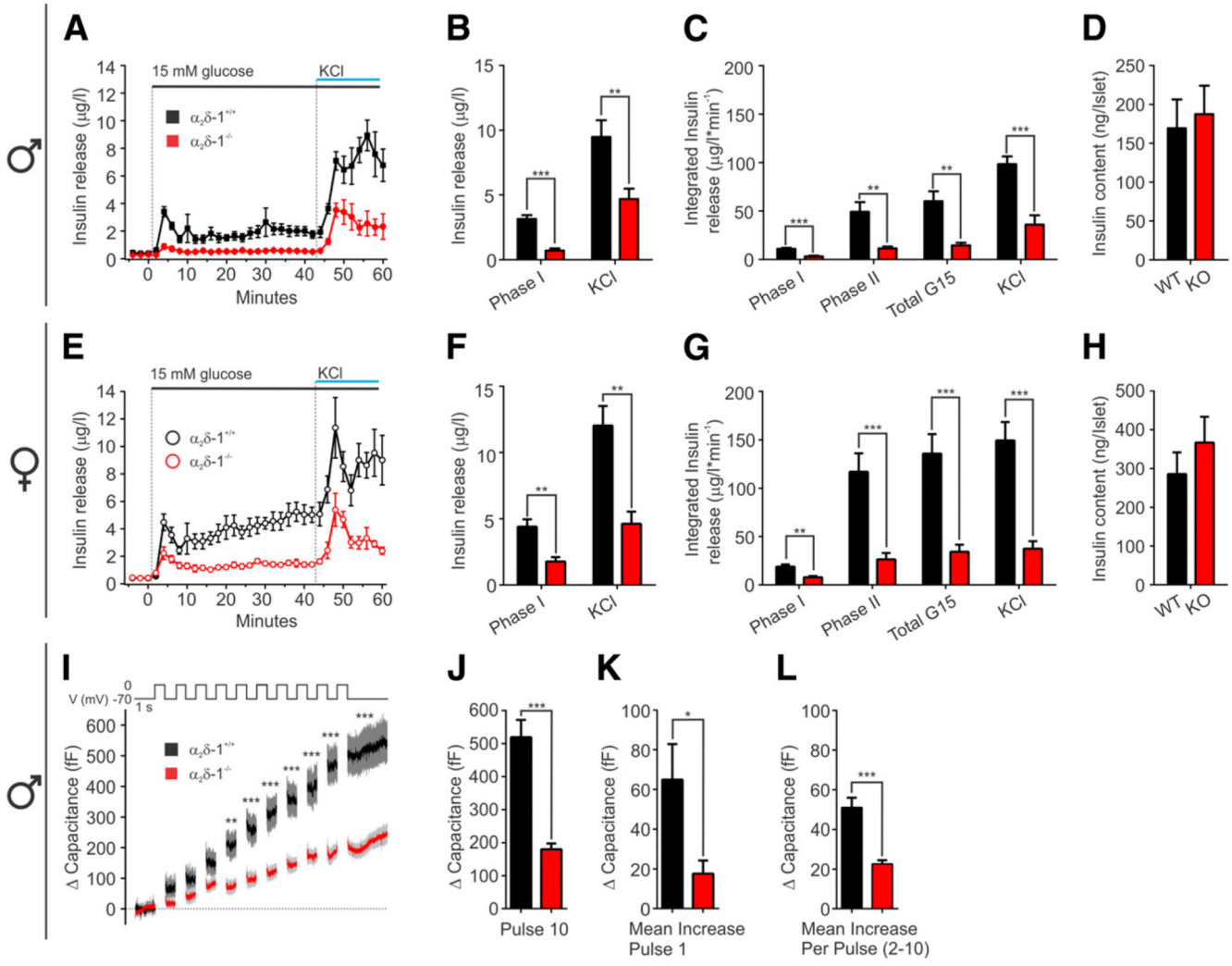

Figure 7.

Deletion of $\alpha_2\delta\text{-}1^{-/-}$ reduces both phases of insulin release. Average insulin secretion from male islets (WT and $\alpha_2\delta\text{-}1^{-/-}$ $n = 6$) (*A*) and female islets (WT $n = 6$, $\alpha_2\delta\text{-}1^{-/-}$ $n = 7$) (*E*). The peak of the first-phase glucose-induced and of KCl-triggered insulin secretion from male (*B*) and female (*F*) islets. Integral of the insulin secretion during the different phases from male (*C*) and female (*G*) islets. Islet insulin content in males (WT $n = 6$, $\alpha_2\delta\text{-}1^{-/-}$ $n = 7$) (*D*) and females (WT $n = 6$, $\alpha_2\delta\text{-}1^{-/-}$ $n = 10$) (*H*). *I*: Average exocytosis evoked by a train of 10 depolarization pulses, 500 ms long, from 270 to 0 mV in WT ($n = 25$, three mice) and $\alpha_2\delta\text{-}1^{-/-}$ ($n = 24$, three mice). *J*: Average capacitance increase after 10 depolarization pulses. *K*: Capacitance increase after the first depolarization pulse. *L*: Mean capacitance increase with each depolarization pulse (pulse 2–10). All values are means ± SEM. Statistics with Student t test: $*P < 0.05$; $**P < 0.01$; $***P < 0.001$.

Europe PMC Funders Author Manuscripts